Can a conceptual model of fluid focusing explain lower-crustal conductors?

Matthew J. Comeau[1], M. Becken[1], A. Grayver[2], J. Käufl[2], A. Kuvshinov[2]

1) Universität Münster, Germany 2) ETH-Zürich, Switzerland

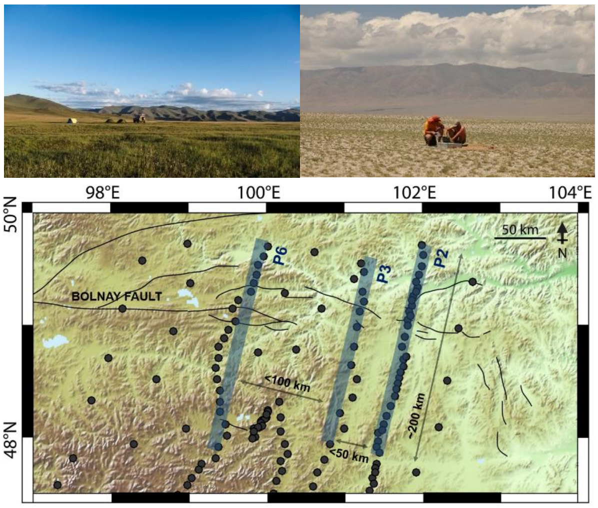

Figure 1: Top: Photographs from magnetotelluric (MT) measurement campaign in Mongolia. **Bottom:** Map of the study area, Bolnay region, central Mongolia. Location of MT measurement sites (circles; see Käufl et al., 2019; Comeau et al., 2018). Here we focus on three profiles (grey bands), ~200 km long and separated by 50-100 km; P6 has 21 sites and an average spacing of ~10 km, P3 has 13 sites and spacing of 7-18 km, P2 has 30 sites and spacing of 3-11 km. Black lines mark fault segments (Calais et al., 2003; Walker et al., 2007).

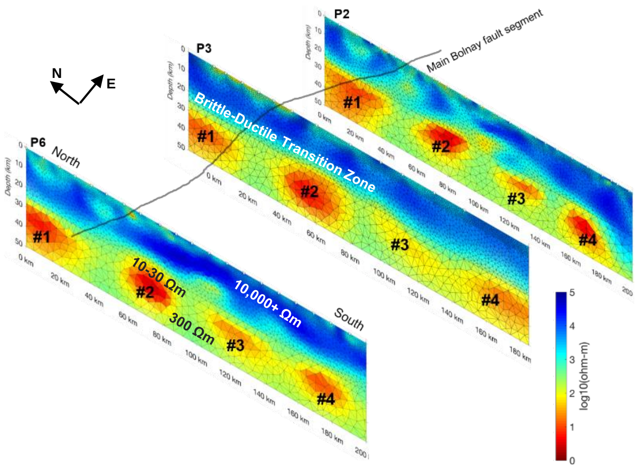

Figure 2: Oblique view of three 2-D resistivity models created with the algorithm of MARE2DEM (Key et al., 2016). Full inversion details (parameters, testing, etc.) and data fit are presented elsewhere. Anisotropic modelling can not explain the model. The upper crust (<25 km) is highly resistive (10,000+ Ωm); explained by the Pre-Cambrian craton of the Hangai Block (Cunningham, 2001). Below the Brittle-Ductile Transition Zone (BDTZ; depth of 15-25 km), anomalous isolated conductors (#1-4; 10-30 Ωm) are embedded in a moderately resistive layer (~300 Ωm). They are interpreted to be zones of interconnected fluids. They appear to be a consistent shape, size, and separation. They appear to be elongated features, parallel to the main Bolnay fault segment (roughly east-west). The fault shows only near-surface conductive anomalies.

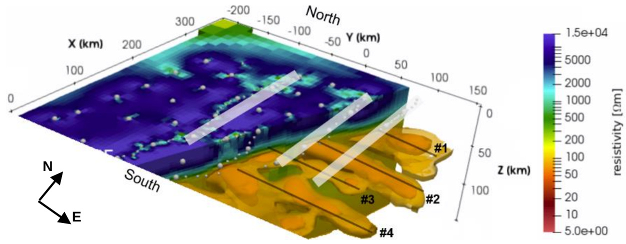

Figure 3: A full 3-D model (Käufl et al., 2019) confirms the elongated tube shape of the anomalies.

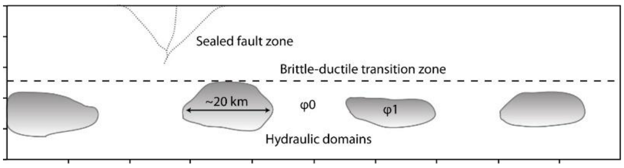

Figure 4: Schematic of resistivity model section. The conductive anomalies, interpreted to be hydraulic domains: are oblate in shape, have width of 20-25 km, thickness of 5-10 km (bottom not well resolved with MT), located ~5 km below the BDTZ, have a resistivity contrast from surroundings of roughly 10:1, have an elongated tube shape in 3-D. Some heterogeneity observed between domains and across profiles. Furthermore, the fault appears to be independent, that is no lower crustal fluid drainage occurs to the fault; it is sealed. All of these features can be explained by a Hydromechanical Model for Lower Crustal Fluid Flow, as proposed by Connolly and Podlachikov (2012; 2017).

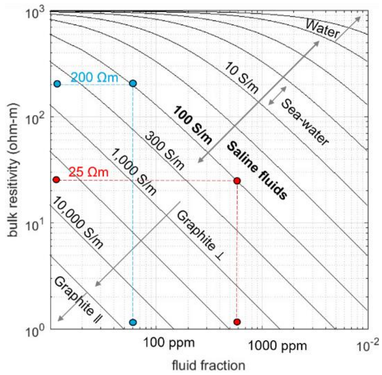

Figure 5: Two-phase equation used to estimate fluid fraction in the lower crust and within the hydraulic domains (Hashin and Shtrikman, 1962). Saline fluids are though to exist in the lower crust, with 100 S/m plausible (Manning, 2018). Case A (hydraulic domains; red): Conductor of 25 Ωm requires fluid content of 600 ppm (0.06%) to explain electrical data. Case B (fluid-poor background; blue): Conductor of 200 Ωm requires fluid content of 60 ppm to explain electrical data. Note: interconnected zones of fluid also significantly lowers the viscosity.

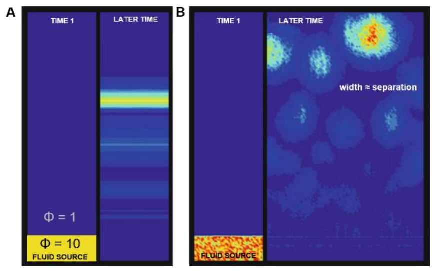

Lower crustal fluid is produced by a source. For example, metamorphic devolatilization reactions generate fluids (e.g., Manning, 2018). Fluids are then distributed along grain edges and form a hydraulically connected network. The fluid propagates upwards because of a pressure gradient; it is expelled by ductile compaction at the bottom (effectively “squeezed” upwards) (Connolly and Podlachikov, 2004). This causes a high porosity region to separate from the source region. Because crustal stress profiles have inverted pressure gradient below the BDTZ, fluids stall 4-10 km below (Connolly and Podlachikov, 2004). This explains the observed location of the “trapped” fluids in the lower crust.

Figure 6: Numerical models modified from Connolly and Podlachikov (2012). Panel A shows an initial porosity distribution that is smooth; 1-D sill-like waves propagate from the source. Panel B shows an initial porosity distribution that is random; 2-D circular waves propagate from the source. These flatten to oblate ellipsoids as they stagnate at the BDTZ barrier. This numerical model shows spatial focusing of the source fluid: the fluid will self-organize into dynamic hydraulic domains of higher porosity. The fluid focusing is a consequence of heterogeneity in the porosity distribution. This may be due to a lithological heterogeneity, or to variations in fluid production. In 3-D, the fluid zones are predicted to be spherical. However, their pattern must be superimposed on: 1) pre-existing crustal heterogeneities (e.g., faults, lithological variations, terrane boundaries), and 2) large-scale deformation pattern from far-field stress (tectonic motion).

$$\delta = \sqrt{(\eta_s / \varphi_0^3 \cdot k_0 / \eta_f)}$$

Compaction length scale (Connolly and Podlachikov, 2017)

Porosity–permeability relationship (Carman–Kozeny, 1927/37)

$$k = \varphi^3 \cdot d_g^2 / (c_\varphi \cdot (1 - \varphi)^2)$$

- η_s effective viscosity of rock matrix
- η_f viscosity of pore fluid
- φ_0 porosity, background value
- k_0 permeability, background value
- φ_1 porosity within fluid domain
- d_g grain size
- c_φ material constant

Figure 7: Hydraulic domain size is controlled by the fundamental compaction length scale (δ), which is a function of rock rheology and fluid properties (Connolly and Podlachikov, 2017). MT measurements give porosity; rock viscosity can be geophysically estimated (e.g., post-seismic slip measurements); pore fluid viscosity is known from experiments; permeability values cover a narrow range and can be computed from theoretical and experimental considerations. We estimate maximum width≈10·δ and thickness≈2·δ. Therefore, in this case, the prediction for hydraulic domain size is: width of ~22 km and thickness of ~5 km. This matches very well with the observations from the MT-derived resistivity model. Therefore, fluid-focusing may be an explanation for the lower crustal conductors below the Bolnay zone, Mongolia.

Citations

Käufl, J., Grayver, A., Comeau, M.J., et al. (2019) Magnetotelluric multiscale 3-D inversion reveals crustal and upper mantle structure beneath the Hangai and Gobi-Altai region in Mongolia. GJI.
Comeau M.J., Käufl, J., Becken, M., et al. (2018) Evidence for fluid and melt generation in response to an asthenospheric upwelling beneath the Hangai Dome, Mongolia. EPSL 487:201-209.
Calais E., Vernolle, M., Sankov, et al. (2003). GPS measurements of crustal deformation in the Baikal-Mongolia area (1994–2002): Implications for current kinematics of Asia. JGR 108:1-14.
Walker, R.T., Nissen, E., Molor, E., et al. (2007) Reinterpretation of the active faulting in central Mongolia: Geology 35:759-762.
Key, K. (2016) MARE2DEM: a 2D inversion code for controlled-source electromagnetic and magnetotelluric data. GJI 207:571-588.
Cunningham, W.D. (2001) Cenozoic normal faulting and regional doming in the southern Hangay region, Central Mongolia: implications for the origin of the Baikal rift province. Tectonophysics 331.
Connolly, J., Podlachikov, Y. (2004) Fluid flow in compressive tectonic settings: implications for midcrustal seismic reflectors and downward fluid migration. JGR 109.
Connolly, J., Podladchikov, Y. (2012) A hydromechanical model for lower crustal fluid flow. In: Metasomatism and the Chemical Transformation of Rock (Harlov, Austrheim), pp. 599–658. Springer.
Connolly, J., Podladchikov, Y. (2017) An analytical solution for solitary porosity waves: implications for dynamic permeability and fluidization of nonlinear viscous and viscoplastic rock. Geofluids 15.
Hashin, Z., Shtrikman, S. (1962) A variational approach to the elastic behavior of multiphase minerals. J. Mech. Phys. Solids 11:127–140.
Manning, C. (2018) Fluids of the Lower Crust: Deep Is Different. Annual Review of Earth and Planetary Sciences 46:67-97.